fermentation

MDPI

Article

Optimization of Palm Kernel Cake Bioconversion with *P. ostreatus*: An Efficient Lignocellulosic Biomass Value-Adding Process for Ruminant Feed

Aldo Ibarra-Rondón [1,*], Dinary Eloisa Durán-Sequeda [1], Andrea Carolina Castro-Pacheco [1], Pedro Fragoso-Castilla [1], Rolando Barahona-Rosales [2] and José Edwin Mojica-Rodríguez [3]

[1] Departamento de Microbiología, Universidad Popular del Cesar, Valledupar 200004, Colombia; deloisaduran@unicesar.edu.co (D.E.D.-S.); andreaccastro@unicesar.edu.co (A.C.C.-P.); pedrofragozo@unicesar.edu.co (P.F.-C.)
[2] Departamento de Producción Animal, Universidad Nacional de Colombia Sede Medellín, Medellín 050034, Colombia; rbarahonar@unal.edu.co
[3] Corporación Colombiana de Investigación Agropecuaria (AGROSAVIA), Agustín Codazzi 202050, Colombia; jmojica@agrosavia.co
* Correspondence: aldoibarra@unicesar.edu.co

Abstract: This study aims to optimize the bioconversion of palm kernel cake (PKC) by *Pleurotus ostreatus* to improve fungal biomass production, lignocellulolytic enzyme expression, and the nutritional value of the substrate as ruminant feed. Three inorganic nitrogen sources (ammonium sulfate, ammonium nitrate, and urea) were evaluated for fungal biomass production using a central composite design (CCD) in liquid fermentations. The formulated culture medium (18.72 g/L glucose and 0.39 g/L urea) effectively yielded better fungal biomass production (8 g/L). Based on these results, an extreme vertex design, mixtures with oil palm by-products (PK, hull, and fiber) supplemented with urea, were formulated, finding that PKC stimulated the highest biomass production and laccase enzyme activity in *P. ostreatus*. The transcriptome of *P. ostreatus* was obtained, and the chemical composition of the fermented PKC was determined. Transcriptomic analysis revealed the frequency of five key domains with carbohydrate-activated enzyme (CAZy) function: GH3, GH18, CBM1, AA1, and AA5, with activities on lignocellulose. In the fermented PKC, lignin was reduced by 46.9%, and protein was increased by 69.8%. In conclusion, these results show that urea is efficient in the bioconversion of PKC with *P. ostreatus* as a supplement for ruminants.

Keywords: white-rot fungi; value-added products; gene expression patterns; lignocellulolytic enzymes; optimization experimental design

Academic Editors: Amina Moss, Weilong Wang and Yukun Zhang

Received: 25 March 2025
Revised: 22 April 2025
Accepted: 23 April 2025
Published: 1 May 2025

Citation: Ibarra-Rondón, A.; Durán-Sequeda, D.E.; Castro-Pacheco, A.C.; Fragoso-Castilla, P.; Barahona-Rosales, R.; Mojica-Rodríguez, J.E. Optimization of Palm Kernel Cake Bioconversion with *P. ostreatus*: An Efficient Lignocellulosic Biomass Value-Adding Process for Ruminant Feed. *Fermentation* **2025**, *11*, 251. https://doi.org/10.3390/fermentation11050251

1. Introduction

Bioconversion of oil palm lignocellulose biomass by *Pleurotus ostreatus* for ruminant feeding purposes involves optimizing fermentation conditions, particularly the carbon and nitrogen availability in the substrate [1]. These conditions directly influence the production and activity of enzymes responsible for degrading anti-nutritional compounds and releasing valuable components for animal nutrition [2]. A study suggested that the regulation of enzyme synthesis in white-rot fungi (WRF) depends on the supply of nitrogen sources in the culture medium, particularly in fermentative processes of lignocellulolytic substrates [3]. Palm kernel cake (PKC) is a high-fiber, medium-grade protein feed with a lignin content between 14–20%, holocellulose of 60%, and crude protein ≈20%, representing a C:N ratio

of 20:1 approximately [4–7]. These concentrations suggest that fungal growth could be favored by the amount of protein contained in the PKC rather than in other residues; thus, this by-product seems sufficient as the only C and N source for its bioconversion into fungal biomass. However, experience shows that not supplying an external nitrogen source to the fermentation process with *P. ostreatus* would mean considerable decreases in crude protein in the by-products. This is possibly because *P. ostreatus* synthesizes proteases [8], which can hydrolyze the protein nitrogen reserves in the residues, and this is undesirable if they are to be used as animal feed. Therefore, the expression of genetic profiles in *P. ostreatus* is a function of the chemical composition of the growth medium, particularly the C:N ratio, which is a key factor that affects the quality of the final product used in animal nutrition programs [9,10]. This highlights the importance of supplementing the medium with nitrogenous nutrients for optimal fungal growth and colonization. Nitrogen metabolite repression (NMR) in filamentous fungi—a regulatory system that controls the expression of enzymes needed to utilize various secondary nitrogen sources—is specifically activated under nitrogen-sufficient conditions, especially when ammonium (NH_4^+) or L-glutamine are present as the nitrogen source [11,12]. Supplementation with nitrogen-rich sources has been shown to enhance the production of lignolytic enzymes and fungal biomass in *P. ostreatus* [13].

The CAZy database (www.cazy.org), supported by results from omics studies, provides information on two categories of WRF-expressed proteins involved in lignocellulose degradation—first, associated modules, and second, catalytic modules. The first category corresponds to carbohydrate-binding modules (CBMs); the second is composed of five enzyme subgroups that have been reported: glycoside hydrolases (GH), glycosyltransferases (GT), polysaccharide lyases (PL), carbohydrate esterases (CE), and auxiliary activities (AA) [14]. CBM, GH, GT, PL, and CE are involved in the hydrolysis of carbohydrates such as cellulose and hemicellulose. The AA group includes lignin-modifying enzymes (LME) and lytic polysaccharide monooxygenases (LPMO) that depolymerize lignin. This last group is the most frequent CAZy found in *P. ostreatus* [15], mainly because this fungus selectively degrades lignin, with a minor effect on cellulose and hemicellulose under nitrogen-sufficient conditions [16,17]. Under these considerations, it is important to identify favorable carbon and nitrogen concentrations in the medium that favor biomass production and lignolytic enzymatic synthesis in *P. ostreatus*, improving the fermentation of lignocellulosic materials.

Statistical designs of experiments, in particular the central composite and the extreme vertex mixture design, have been consolidated as effective approaches to improve the interpretation of how interactions between nutritional factors regulate growth and enzyme production in *P. ostreatus* [13], as well as to reduce process times and costs [18]. In this study, an central composite design (CCD) and extreme vertex were used to optimize the culture medium C:N ratio with different sources of inorganic nitrogen that enhances mycelial development, and the expression of enzyme genes related to carbohydrate metabolism (lignocellulose) by *P. ostreatus*, improving the fermentation process and generating added value to oil palm by-products.

2. Materials and Methods

2.1. Optimization of Biomass Production Using a Central Composite Design (CCD)

A commercial strain of *P. ostreatus* (genetically compatible with *P. ostreatus* PC15_PC15) maintained on malt extract agar at 4 °C was used. The inoculum consisted of 4-mm diameter agar discs from the peripheral growth area of the fungus incubated at 25 °C for eight days on malt extract agar; one agar disc with mycelium was used to inoculate 20 mL of liquid culture medium. The concentrations of glucose and inorganic nitrogen sources

(ammonium sulfate, ammonium nitrate, and urea) were defined according to a two-factor two-level composite central design (CCD). Here, the factors to be evaluated corresponded to the glucose concentration and the concentration of the inorganic nitrogen source at the high and low levels (Table 1). Thirteen culture media formulations were obtained (Table 2) after defining the high and low levels of the factors in the CCD. The CCD allows estimation of the curvature of a response surface for a specific variable and calculation of the terms of a first or second-order model.

Table 1. Factors and levels of the central composite design 2^k.

Factor	Low Level	High Level
[g/L] Glucose	−1	1
[g/L] Inorganic Nitrogen	−1	1

Submerged culture fermentations (SmF) of 100 mL of culture medium were carried out in 250 mL flasks at 25 °C ± 2 °C and 150 rpm for 13 days [19]. Ammonium sulfate ($(NH_4)_2SO_4$), ammonium nitrate (NH_4NO_3), and urea (CH_4N_2O) were used as sources of inorganic nitrogen. Glucose and 0.4 g/L^{-1} of yeast extract were used as the basal ingredients of the medium to achieve different carbon-to-nitrogen (C:N) ratios under the experimental conditions (Table 2). All SmF cultures were inoculated with five 4-mm diameter discs taken from the growth zone of eight-day-old cultures of *P. ostreatus*.

Table 2. Calculated concentrations of glucose and inorganic nitrogen for a CCD 2^k.

Medium	Glucose [g/L^{-1}]	Inorganic Nitrogen [g/L^{-1}]	Yeast Extract [g/L^{-1}]	C:N Ratio
GASYE1	13	0.1	0.4	5:1
GASYE2	3.7	0.1	0.4	81:1
GASYE3	1.3	0.5	0.4	6:1
GASYE4	3.7	0.5	0.4	16:1
GASYE5	0.8	0.3	0.4	6:1
GASYE6	4.2	0.3	0.4	31:1
GASYE7	2.5	0.02	0.4	321:1
GASYE8	2.5	0.6	0.4	9:1
GASYE9	2.5	0.3	0.4	18:1
GASYE10	2.5	0.3	0.4	18:1
GASYE11	2.5	0.3	0.4	18:1
GASYE12	2.5	0.3	0.4	18:1
GASYE13	2.5	0.3	0.4	18:1
GANYE1	12.5	1.5	0.4	4:1
GANYE2	37.5	1.5	0.4	11:1
GANYE3	12.5	5.5	0.4	1:1
GANYE4	37.5	5.5	0.4	3:1
GANYE5	7.3	3.5	0.4	1:1
GANYE6	42.7	3.5	0.4	5:1
GANYE7	25	0.67	0.4	17:1
GANYE8	25	6.32	0.4	2:1
GANYE9	25	3.5	0.4	3:1
GANYE10	25	3.5	0.4	3:1
GANYE11	25	3.5	0.4	3:1
GANYE12	25	3.5	0.4	3:1
GANYE13	25	3.5	0.4	3:1

Table 2. *Cont.*

Medium	Glucose [g/L^{-1}]	Inorganic Nitrogen [g/L^{-1}]	Yeast Extract [g/L^{-1}]	C:N Ratio
GUYE1	12.5	0.5	0.4	18:1
GUYE2	25	0.5	0.4	36:1
GUYE3	12.5	1	0.4	9:1
GUYE4	25	1	0.4	18:1
GUYE5	9.9	0.8	0.4	9.4:1
GUYE6	27.6	0.8	0.4	26.3:1
GUYE7	18.8	0.4	0.4	34:1
GUYE8	18.8	1.1	0.4	12.2:1
GUYE9	18.8	0.8	0.4	18:1
GUYE10	18.8	0.8	0.4	18:1
GUYE11	18.8	0.8	0.4	18:1
GUYE12	18.8	0.8	0.4	18:1
GUYE13	18.8	0.8	0.4	18:1

GASYE: glucose + ammonium sulfate + yeast extract; GANYE: glucose + ammonium nitrate + yeast extract; GUYE: glucose + urea + yeast extract.

The elemental composition analysis of the yeast extract used in this study showed an estimated C:N ratio of 4:1; while for urea, the C:N ratio was 0.43:1.

The biomass was measured gravimetrically. For this purpose, the known culture volume was filtered through filter paper (dried and weighed previously). The filter with the retained material was dried at 70 °C for 24 h [20].

2.2. Extreme Vertex Design for Biomass Production in Solid Fermentation Using Oil Palm By-Product Blends

The solid-state fermentation (SSF) systems design was carried out using an experimental extreme vertex mixing design. The C:N ratio of each formulation was adjusted based on the composition that yielded the highest fungal biomass production under SmF, using urea as the selected inorganic nitrogen source. The mixtures were adjusted to 60% moisture content and an initial pH of 5.5, followed by sterilization at 121 °C and 120 kPa for 15 min. After sterilization, the substrate was aseptically inoculated at a rate of 4% (dry matter basis) using 4-mm diameter pellets of *Pleurotus ostreatus* and incubated at 30 °C for 13 days under dark conditions [21]. To facilitate aerobic metabolism during the incubation, the bags were sealed with a semi-permeable adhesive membrane that allowed gas exchange. Upon completion of the incubation period, the fermented material was dried at 50 °C for 48 h. The components of the mixtures were palm kernel, fiber and hulls, and urea. The amounts established for the blends are shown in Table 3.

Table 3. By-product amounts in the extreme vertex design.

Order	Block	Palm Kernel Cake (g)	Fiber (g)	Palm Kernel Shells (g)
1	1	40	0	0
2	1	0	40	0
3	1	0	0	40
4	1	20	20	0
5	1	20	0	20
6	1	0	20	20
7	1	13.33	13.33	13.33
8	1	27	6.5	6.5
9	1	6.5	27	6.5
10	1	6.5	6.5	27

The elemental composition in terms of the C:N ratio of palm kernel cake, fiber, and palm kernel shells was 18:1, 52:1, and 86:1, respectively.

Since, in solid-state fermentation, the fungal biomass of the fungus grows attached to the lignocellulose biomass, the fungal biomass was measured indirectly by quantifying the amount of N-acetyl-D-glucosamine (NAGA), which is a precursor of chitin, a major component of the fungal cell wall [22].

Determination of Laccase Enzyme Activity

The evaluation of laccase activity was carried out following the methodology of Zhou et al. [23]. For this, 1 g of the fermented residue was suspended in 9 mL of distilled water and incubated at 200 rpm for 10 min. Subsequently, the suspension was centrifuged at 4000 rpm for 15 min. Next, 5 µL of the supernatant was taken and mixed with 1 mL of a 1:100 solution of 2,2′-azinobis-(3-ethylbenzothiazoline-6-sulphonic acid) (ABTS) in sodium citrate buffer (pH 4). Finally, absorbance was measured at 436 nm using a spectrophotometer, as reported by Durán-Sequeda et al. [19].

2.3. Transcriptome Analysis

For transcriptomic analysis, the fungus was grown on the optimized medium, enriched with palm kernel cake at 20 g/L. The media were incubated for 8 days at 28 °C and 200 rpm. At the end of the incubation time, the fungal biomass was separated from the culture medium by filtration on sterile 0.45 µm cellulose paper. 100 ng of biomass was sprayed with liquid nitrogen and immediately suspended in Trizol TM Reagent for RNA extraction. Total RNA extraction was performed following the standard RNA extraction protocol described by the manufacturer (Trizol TM Reagent, Invitrogen, Waltham, MA USA; Total RNA extraction protocol). RNA integrity was measured by calculating the RIN value by capillary electrophoresis. Once the RNA quality was verified, RNA-seq sequencing was carried out. A TruSeq stranded mRNA library was prepared, and 150-base paired reads were read on the Illumina Novaseq 6000 platform (San Diego, CA, USA). CUTADAPT v3.5 was used to clean the reads with a Q30 quality threshold, and reads with ambiguous bases were excluded (Ns). Trinity v2.13.2 with default values was used for de novo transcriptome assembly. The overall statistics of the transcriptome were calculated with a proprietary script written in Python (https://www.python.org/). Functional annotation of the assembled sequences was processed with EggNOG-mapper [24], using stringent parameters for filtering and coverage (E-value $\leq$ 0. 001, minimum score of 60, minimum identity of 40%, and minimum coverage of 20%) which generated GO (Gene Ontology), KEGG (Kyoto Encyclopedia of Genes and Genomes) CAZy (Carbohydrate-Active enZYmes), PFAMs (Protein Families) annotations, the functional description, short name and Enzyme Commission Number (EC) available for each sequence. Additionally, KEGG Mapper Reconstruction of GhostKOALA was used to determine the frequencies of KEGG Categories identified in the transcriptome.

2.4. Determination of the Chemical Composition of PKC Fermented in Urea-Enriched Solid Medium

The PKC, together with the fungal biomass, was dried at 60 °C until a constant weight was reached at the end of the solid-state fermentation. Subsequently, the chemical composition of the fermented substrate in terms of crude protein (CP), neutral detergent fiber (NDF), acid detergent fiber (ADF), and lignin (LIG) was determined by NIRS (near infrared spectroscopy) [25].

2.5. Statistical Analysis

Minitab® 18 was used to construct the statistical design, assess statistical significance, obtain the regression models, and find the simultaneous local optimum of one or more response variables [26].

3. Results and Discussion

3.1. Biomass Production Optimization

Figure 1 shows the results of biomass production of *P. ostreatus* (gL^{-1}) growing in different concentrations of glucose and inorganic nitrogen sources in a liquid medium. CCD results indicated that biomass production was affected by both glucose concentrations and different sources and ratios of inorganic nitrogen in the medium (Figure 1). Maximum biomass production using ammonium sulfate (8 g/L), ammonium nitrate (10.5 g/L), and urea (8 g/L) was obtained at C:N ratios of 10:1, 11:1 and 34:1, respectively (Figure 2), with no significant statistical differences ($p < 0.05$). However, it is suggested that the nitrogen available in urea is more assimilable by the fungus for biomass production, given the higher C:N ratio needed to produce a similar amount of biomass to that of the other nitrogen sources (Figure 2).

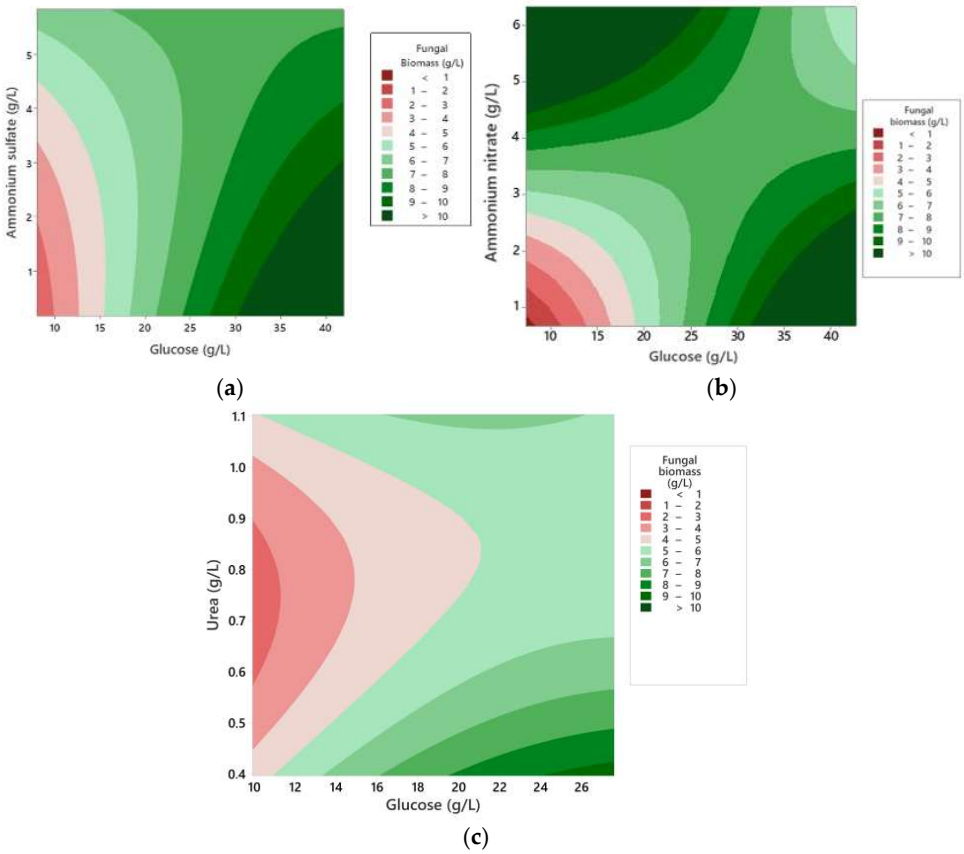

Figure 1. Boundary plots of biomass production of *P. ostreatus*. (**a**) Culture at different concentrations of ammonium sulfate. (**b**) Culture at different concentrations of ammonium nitrate. (**c**) Culture at different concentrations of urea.

These findings indicate that urea provides a higher amount of assimilable nitrogen in the form of ammonia, facilitating a faster and more efficient uptake of nitrogen, supporting increased cell growth, and, consequently, greater biomass accumulation [27]. Furthermore, the high ratio of carbon to nitrogen in the case of urea may allow for an optimal balance between energy availability and nitrogen supply, which is crucial for the synthesis of

essential biomolecules such as proteins and nucleic acids. This balance could explain why urea, although requiring a higher C ratio, is more effective in promoting the biomass production of *P. ostreatus*.

(**a**) (**b**) (**c**)

Figure 2. Maximum biomass production of *P. ostreatus*. (**a**) Synthetic with ammonium sulfate (glucose 41.97 g/L and ammonium sulfate 3 g/L) results in 8 g/L of biomass, and a C:N ratio of 10.3:1. (**b**) Synthetic with ammonium nitrate (glucose 37.5 g/L and ammonium nitrate 1.5 g/L) results in 10.5 g/L of biomass and a C:N: ratio of 11:1. (**c**) Synthetic with urea (glucose 18.72 g/L and urea 0.39 g/L) results in 8 g/L of biomass and a C:N: ratio of 34:1.

Some authors have reported that supplementing the substrate with urea not only increases the productivity of *P. ostreatus* but also enhances its nutritional value, particularly in terms of protein and β-glucans [28]. A recent study found that growing *P. ostreatus* on a spent oyster substrate mixed with wheat straw (1:1, *w*/*w* mixture) enriched with urea in doses between 3g and 5g per kilogram of substrate increased the protein and essential amino acid contents of the fungus, reaching up to 0.8% and 0.31%, respectively [29]. This suggests a significant improvement in the nutritional value of *P. ostreatus*.

Using response surface methodology, another study identified that the optimal urea concentrations for higher laccase enzyme production in *P. ostreatus* were between 0.8% and 1.2% (*w*/*v*), similar to the findings observed in this research regarding biomass production [30]. When evaluating the effects of four lignocellulolytic substrates and urea dosage on the growth and yield of *P. ostreatus*, Déo, and Faustin [31] found that the highest yield and mushroom diameter were observed with a corn cob substrate supplemented with 100 g of urea per kg of substrate. This dose is significantly higher than that reported in this study, possibly due to differences in experimental conditions, such as substrate variety, mushroom species, or nutrient availability, all of which may influence the response to urea fertilization.

In this regard, the use of urea as a source of inorganic nitrogen for *P. ostreatus* growth maximizes fungal biomass production. It presents an economical and easy-to-use alternative compared to other inorganic nitrogen sources evaluated in this study, making it a preferred option for large-scale production of mycelial protein from *P. ostreatus*.

3.2. Biomass Production and Laccase Enzyme Activity in Solid-State Fermentation

In Figure 3, each vertex of the triangle represents one of the three components of the mixture. The figure shows 10 points in the design space, corresponding to the mixtures defined in Table 3. The data indicate that both fungal biomass (2.4 g/L) and laccase enzyme activity (1200–1400 U/L) reached the highest values in the mixtures with the highest proportion of palm kernel cake. This suggests that fungal growth may benefit from the higher amount of protein present in the palm kernel cake compared to fiber and kernel hulls. Therefore, this by-product seems to be a suitable option for bioconversion into fungal biomass.

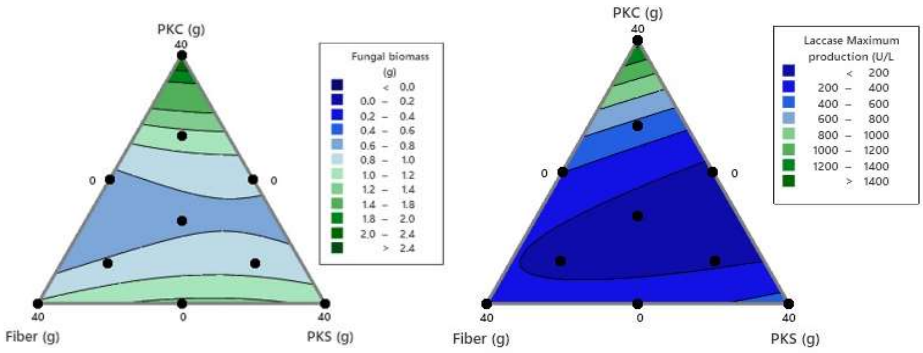

(**a**) (**b**)

Figure 3. (**a**) Mixing boundary plot of maximum biomass production and (**b**) maximum laccase enzyme production of *P. ostreatus* growing on urea-enriched oil palm by-product mixtures. PKC: palm kernel cake; PKS: palm kernel shells.

Recent studies have also shown that urea is an efficient source of inorganic nitrogen, stimulating growth and ligninolytic enzyme synthesis in *P. ostreatus* [32,33]. Additionally, urea supplementation not only stimulates the growth of WRF but also enhances lignin degradation by increasing the activity of ligninolytic enzymes, thus promoting the bioconversion of lignocellulosic residues [34].

3.3. Transcriptomic Analysis

Identification of metabolic pathways activated in *P. ostreatus* under urea- and palm kernel cake-enriched conditions, related to the fungus's ability to bioconvert lignocellulosic and metabolic components, was carried out. 7029 KEGG_ko terms were filtered from the genome with 13,635 coding fragments, and the frequency of each unique term (3167) was established. Table 4 presents the top 20 most frequent terms, totaling 389 annotations, and Figure 4 the most frequent domains. The results show a clear activation of carbohydrate metabolism, highlighting proteins associated with complex polysaccharide hydrolytic pathways such as chitinase (K01183) and B-glucosidase (K05349) with the highest frequencies, of 26 and 24, respectively; as well as cellulose 1,4-B-cellobiosidase (K01225) and pectate lyase (K01728). Unclassified metabolic pathways also support this activity, as oxidative proteins like glyoxal oxidase (K20929) and lytic cellulose monooxygenase (K19356) are frequently found and are key for lignin degradation [35,36]. Similarly, the activation of xenobiotics metabolism is highlighted, with enzymes like salicylate hydroxylase (K00480) and microsomal epoxide hydrolase (K01253) showing capabilities in degrading aromatic or toxic compounds derived from the processing of lignin's aromatic monomers [37,38]. These results show that *P. ostreatus* is highly efficient in the molecular activation of enzymes involved in the bioconversion of agro-industrial wastes such as palm kernel cake.

Table 4. Top 20 most frequent KEGG terms in the transcriptome of *P. ostreatus* grown in GY medium enriched with urea and palm kernel cake.

KEGG Orthology	Protein Name	K Number	Frequency
Carbohydrate metabolism	Chitinase	K01183	26
Carbohydrate metabolism	B-glucosidase	K05349	24
Carbohydrate metabolism	Cellulose 1,4-B-cellobiosidase	K01225	18
Carbohydrate metabolism	Aldehyde dehydrogenase	K00128	18
Carbohydrate metabolism	Alpha-galactosidase	K07407	18
Carbohydrate metabolism	Succinate dehydrogenase	K00237	17
Carbohydrate metabolism	Pectate lyase	K01728	14
Unclassified: metabolism	Glyoxal oxidase	K20929	23

Table 4. *Cont.*

KEGG Orthology	Protein Name	K Number	Frequency
Unclassified: metabolism	Lytic cellulose monooxygenase	K19356	22
Unclassified: metabolism	NADPH2 dehydrogenase	K00354	18
Unclassified: metabolism	Protein-serine/threonine kinase	K08286	15
Xenobiotics biodegradation and metabolism	Salicylate hydroxylase	K00480	24
Xenobiotics biodegradation and metabolism	Microsomal epoxide hydrolase	K01253	16
Xenobiotics biodegradation and metabolism	Cyclohexanone monooxygenase	K03379	15
Glycan biosynthesis and metabolism	Mannosyl-oligosaccharide alpha-1,2-mannosidase	K01230	16
Lipid metabolism	Glycerol 2-dehydrogenase	K18097	26
Metabolism of other amino acids	Glutathione S-transferase	K00799	15
Amino acid metabolism	Choline dehydrogenase	K00108	31
Mitochondrial biogenesis	Mitochondrial chaperone BCS1	K08900	15
Signal transduction	cathepsin D	K01379	18

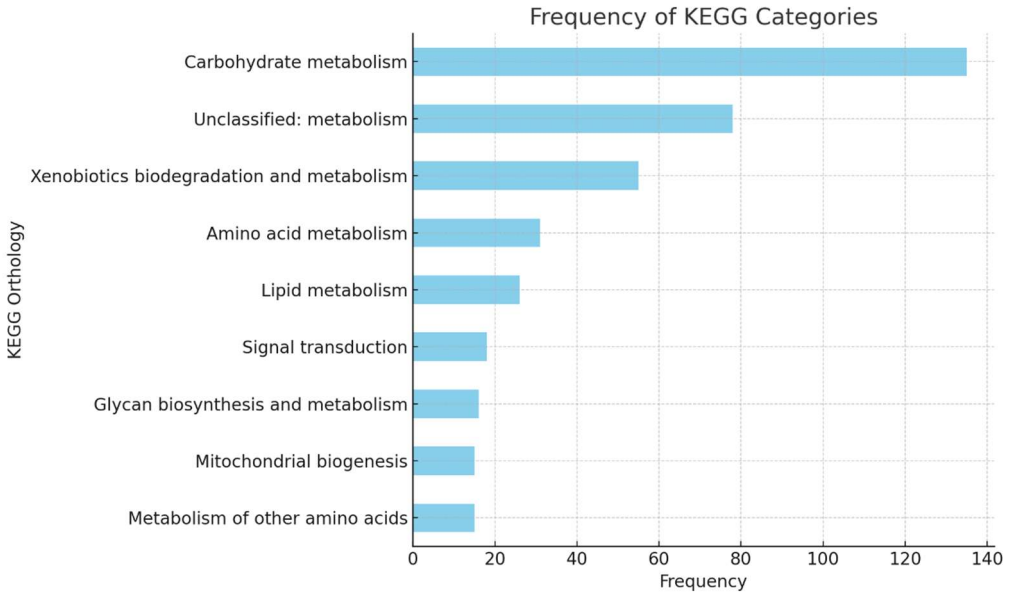

Figure 4. Frequency of KEGG categories identified in the transcriptome of *P. ostreatus* grown on GY medium enriched with urea and palm kernel cake.

Table 5 presents a comparison between the CAZymes identified in *P. ostreatus* transcriptome and frequencies reported in the literature, aiming to explore similarities and recurrent patterns across different studies and experimental contexts. While the frequencies in both cases are not directly comparable due to differences in methodologies and experimental conditions, the results highlight consistent trends that reinforce the relevance of certain CAZymes in the degradation of lignocellulosic substrates. On one hand, the frequencies reported in the transcriptome (405 genes identified) specifically reflect gene expression under the current experimental conditions (urea-enriched medium and palm kernel cake). On the other hand, the frequencies in the literature represent an aggregate of several studies (n = 9) *, covering different experimental conditions, methodologies (transcriptome, secretome, proteome), and lignocellulosic substrates. In both datasets (Table 5), the most frequently reported domains are related to holocellulose: GH3, GH7, CBM1, and AA9 are prominent in both lists and suggest their key role in cellulose and hemicellulose hydrolysis. For lignin degradation, AA1, AA2, AA3, and AA5 stand out, reinforcing *P. ostreatus*'s ability to depolymerize lignin through oxidative pathways. These findings indicate that the most

relevant enzymes in lignocellulosic processing are consistently expressed under various experimental conditions.

Table 5. Frequencies of CAZymes identified in the transcriptome of *P. ostreatus* and comparison with published literature on lignocellulosic substrates.

CAZys	Main Lignocellulose Substrate	Frequency in the Transcriptome	Frequency in the Literature *
AA1	Lignin	15	23
AA2	Lignin	14	15
AA3	Lignin	11	13
AA4	Lignin	NR	1
AA5	Lignin	24	11
AA6	Lignin	2	3
AA7	Lignin	NR	1
AA8	Lignin	NR	1
AA9	Holocellulose	22	5
CBM1	Holocellulose	25	9
CBM13	Holocellulose	NR	1
CBM21	Holocellulose	NR	1
CBM48	Holocellulose	2	NR
CE	Hemicellulose/pectin	NR	1
CE1	Hemicellulose/pectin	1	3
CE10	Hemicellulose/pectin	3	1
CE16	Hemicellulose/pectin	NR	3
CE4	Hemicellulose/pectin	NR	1
GH1	Holocellulose	8	3
GH10	Holocellulose	NR	4
GH105	Holocellulose	3	NR
GH115	Holocellulose	NR	1
GH12	Holocellulose	2	1
GH127	Holocellulose	NR	1
GH128	Holocellulose	NR	1
GH13	Holocellulose	9	NR
GH15	Holocellulose	4	1
GH16	Holocellulose	9	2
GH17	Holocellulose	NR	1
GH18	Chitin	26	NR
GH2	Holocellulose	NR	3
GH20	Holocellulose	2	NR
GH28	Pectin	NR	1
GH3	Holocellulose	32	9
GH30	Holocellulose	5	NR
GH31	Holocellulose	11	1
GH32	Holocellulose	NR	NR
GH35	Holocellulose	NR	6
GH37	Holocellulose	2	NR
GH38	Holocellulose	2	NR
GH39	Holocellulose	NR	1
GH43	Holocellulose	3	1
GH47	Holocellulose	16	3
GH5	Holocellulose	15	5
GH51	Holocellulose	4	6
GH53	Holocellulose	NR	1
GH6	Holocellulose	4	2

Table 5. *Cont.*

CAZys	Main Lignocellulose Substrate	Frequency in the Transcriptome	Frequency in the Literature *
GH63	Holocellulose	NR	1
GH7	Holocellulose	18	4
GH72	Holocellulose	NR	1
GH74	Holocellulose	3	1
GH76	Holocellulose	NR	2
GH78	Holocellulose	NR	1
GH79	Holocellulose	NR	1
GH9	Holocellulose	13	NR
GH90	Holocellulose	NR	1
GH92	Holocellulose	NR	2
GH95	Holocellulose	4	NR
GT1	Holocellulose	5	NR
GT15	Holocellulose	9	NR
GT17	Holocellulose	NR	NR
GT18	Holocellulose	2	NR
GT2	Holocellulose	19	1
GT20	Holocellulose	3	NR
GT21	Holocellulose	NR	NR
GT22	Holocellulose	4	NR
GT24	Holocellulose	NR	NR
GT3	Holocellulose	NR	NR
GT33	Holocellulose	1	NR
GT35	Holocellulose	NR	NR
GT39	Holocellulose	3	NR
GT4	Holocellulose	11	NR
GT41	Holocellulose	2	NR
GT48	Holocellulose	3	NR
GT5	Holocellulose	2	NR
GT50	Holocellulose	1	NR
GT57	Holocellulose	7	NR
GT58	Holocellulose	4	NR
GT59	Holocellulose	2	NR
GT66	Holocellulose	NR	NR
GT69	Holocellulose	1	NR
GT76	Holocellulose	NR	NR
GT8	Holocellulose	9	NR

* [14,15,39–45]. NR: no reported.

Figure 5 illustrates the relationship between the CAZyme domains identified in the *P. ostreatus* transcriptome and those reported in the literature. It shows 23 common domains, including key families such as GH3, GH7, AA9, AA1, and AA5, essential for holocellulose and lignin degradation. The 36 unique domains in the transcriptome suggest specific adaptations to the experimental conditions with palm kernel cake, while the 29 unique domains in the literature reflect methodological and substrate differences used in other studies. This overlap validates the relevance of the identified CAZymes and highlights new opportunities to explore specific enzymes with biotechnological potential in the bioconversion of lignocellulosic residues, positioning *P. ostreatus* as a robust model in this field.

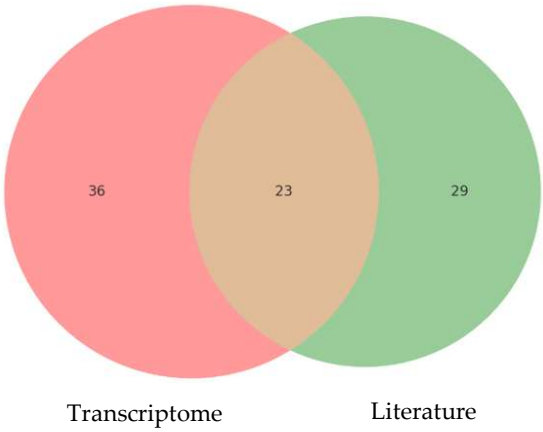

Figure 5. Comparison of CAZyme domains identified in the transcriptome of *P. ostreatus* and reported in the literature.

Figure 6 presents an integrated analysis of the CAZyme domains identified in the *P. ostreatus* transcriptome compared to the frequencies reported in the literature. A summary of the most frequently mentioned domains in previous studies is provided, emphasizing their relevance in lignin, cellulose, and hemicellulose processing. The figure also highlights the most expressed domains in the transcriptome under specific experimental conditions, such as the palm kernel cake enriched medium. Additionally, Figure 6 visualizes key findings, including the high frequency of GH3, AA1, AA5, and CBM1, which validate the experimental results in the context of existing knowledge. Furthermore, unique domains of the transcriptome, such as GH18, were identified, which might reflect specific adaptations to the experimental environment and are primarily involved in the degradation of fungal cell wall components, such as chitin [15,46]. This integration of results underlines both the consistency and novel contributions of the present study, reinforcing the importance of *P. ostreatus* as a model for the bioconversion of lignocellulosic residues.

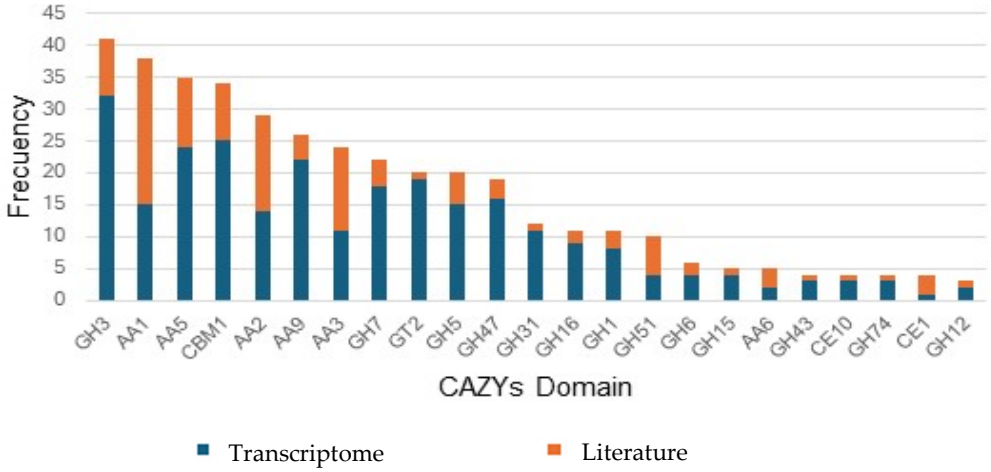

Figure 6. Comparison of CAZyme domains in the transcriptome and the literature.

Based on omics data from the literature and the findings of this study, we propose a general mechanism to elucidate the enzymatic degradation of lignocellulose by *Pleurotus* sp. This mechanism is supported by the structural composition of the lignocellulosic complex, represented by the carbohydrate cellulose and hemicellulose, and the lignin fraction. CBM1 interacts with the cellulose or hemicellulose fraction without exhibiting catalytic activity, thereby enhancing the function of GH7 (which includes EC 3.2.1.4 and cellulose endo-β-1,4-glucosidase). Additional GHs, such as GH3 (including EC 3.2.1.58 and glucan exo-β-1,3-

glucosidase) and GH51 (including EC 3.2.1.8, xylan endo-β-1,4-xylosidase or EC 3.2.1.37, and xylan exo-β-1,4-xylosidase, among others), may contribute to hemicellulose fraction modification. AA9 (EC 1.14.99.54; lytic cellulose monooxygenase) plays a role in cellulose degradation. AA1_1 (laccases) and AA2 (including manganese peroxidase EC 1.11.1.13 and versatile peroxidase EC 1.11.1.16) are classified as LMEs. Hydrogen peroxide (H_2O_2), generated by AA3_2 (which includes aryl alcohol oxidase and glucose 1-oxidase) and AA5_1 (including EC 1.2.3.15, glyoxal oxidase serves as a co-substrate for AA2 and AA9.

Table 6 presents a set of KEGG orthology (KO) genes identified in this study that are potentially involved in the regulation of nitrogen metabolism, particularly in the utilization of urea as a nitrogen source during the growth of *P. ostreatus*.

Table 6. Proposed metabolic pathway for nitrogen assimilation from urea in *Pleurotus ostreatus*, including key enzymes and corresponding KEGG orthologs (KOs).

Step	Protein Name	K Number	Principal Reaction
1	Urease	K01428	Urea → 2 NH_3 + CO_2
2	Glutamine synthetase	K01915	NH_3 + Glutamate + ATP → Glutamine
3	Glutamate synthase (NADH)	K00264	Glutamine + α-Ketoglutarate + NADH → 2 Glutamate
4	Aminotransferases	K01763, K20247	Glutamate + Keto acid → New amino acid → Biomass synthesis

Based on the findings, the proposed pathway for urea assimilation in *P. ostreatus* involves the use of urea as an accessible nitrogen source, which is initially hydrolyzed into ammonia and carbon dioxide by the enzyme urease. The resulting ammonia is then efficiently incorporated into organic molecules through the glutamine synthetase–glutamate synthase (GS-GOGAT) cycle, a high-affinity system essential under low-ammonia conditions. Subsequently, the glutamine produced is converted into glutamate, which acts as a key nitrogen donor in transamination reactions catalyzed by aminotransferases. These reactions enable the incorporation of nitrogen into amino acids and other nitrogen-containing compounds, thereby supporting fungal growth and biomass production. The identification of corresponding KEGG orthologs provides additional evidence supporting the functionality of these enzymatic steps in *P. ostreatus*.

3.4. Changes in the Chemical Composition of PKC Fermented

Table 7 presents the chemical composition of palm kernel cake (PKC), both unfermented (NFPKC) and fermented with *P. ostreatus* (PoFPKC). Liquid fermentation of palm kernel cake with *P. ostreatus* resulted in significant improvements to its nutritional profile, including a 26.3% reduction in neutral detergent fiber (NDF), a 20.4% reduction in acid detergent fiber (ADF), and a 46.9% reduction in lignin (LIG). This indicates that pretreatment of palm kernel cake with *P. ostreatus* facilitates the breakdown of bonds between cellulose, hemicellulose, and lignin, as a result of the lignocellulosic enzymes secreted by the fungus [47], as supported by the transcriptome findings reported in this study.

In a previous study, it was observed that the production of ligninolytic enzymes by *P. ostreatus* significantly impacted the lignocellulosic structure of maize stover, leading to an 18.3% reduction in NDF and a 6.8% reduction in ADF content, along with a 118% increase in non-fiber carbohydrates [48]. Similarly, treatment of oil palm empty fruit bunches (RFV) with WRF, including *Pleurotus* sp., resulted in up to a 20% decrease in lignin content, alongside increases of between 7.49 and 16.67% in cellulose levels [49].

Table 7. Chemical composition of PKC after fermentation with *P. ostreatus*.

Chemical Composition (% MS)	NFPKC	PoFPKC
Crude protein	15.9	27.0
Neutral detergent fiber	67.2	49.5
Acid detergent fiber	40.3	32.1
Lignin	14.5	7.7

NFPKC: non-fermented palm kernel cake; PoFPKC: *Pleurotus ostreatus* fermented palm kernel cake.

Simultaneously, a 69.8% increase in CP content was recorded, which could be attributed to the production of mycelial biomass by the fungus, which is particularly rich in protein [50]. In this regard, protein enrichment of the lignocellulosic substrate occurs because approximately 70% of the nitrogen present in *P. ostreatus* is in the form of protein [51]. Similarly, increases of up to 71% in crude protein content were found in corn cob waste pretreated with *P. ostreatus* [52], while fermentation of maize straw with *Pleurotus* spp. led to an increase in the protein content of up to 38% [17].

In parallel, it has been demonstrated that, beyond improving the nutritional composition of the substrate, the fermentation of lignocellulosic material with *P. ostreatus* enhances the final product with bioactive secondary metabolites. Among these is lovastatin, an inhibitor of the enzyme (3S)-hydroxy-3-methylglutaryl-coenzyme A (HMG-CoA) reductase, which plays a key role in the mevalonate pathway for the synthesis of isoprenoid ether lipid precursors involved in the formation of cell membranes in methanogenic archaea [53]. Lovastatin also interferes with the synthesis of coenzyme F420, which participates in electron transport during methanogenesis, thereby contributing to a reduction in methane production [54]. The presence of this metabolite in palm kernel cake (PKC) may be associated with the identification of KEGG orthologs K05607, K02267, and K00507 in the transcriptomic data from this study, corresponding to the enzymatic activities of enoyl-CoA hydratase/isomerase, cytochrome c oxidase, and cytochrome b5-like heme/steroid-binding domain proteins, respectively.

Therefore, the enrichment of PKC with anti-methanogenic metabolites may represent a sustainable approach to mitigating emissions of enteric methane—a potent greenhouse gas generated during rumen fermentation—without compromising animal nutrition [55,56]. These results support the potential of PoFPKC as a functional feed supplement for ruminants.

4. Conclusions

Optimization of fermentation conditions using statistical methods determined that the use of urea as a source of inorganic nitrogen and palm kernel cake as a by-product improved biomass production and the expression of genes involved in lignocellulose hydrolysis in *Pleurotus ostreatus*. This approach contributes to understanding the biochemical processes that regulate the bioconversion of palm kernel cake into a functional feed enriched with microbial protein from *P. ostreatus* for use in ruminant feed.

Author Contributions: A.I.-R.: conceptualization, resources, methodology, data analysis, writing—original draft, writing—review and editing. D.E.D.-S.: methodology, validation, formal analysis, writing—original draft, data curation, writing—review and editing. A.C.C.-P.: methodology, validation, formal analysis. P.F.-C.: formal analysis, writing—original draft, resources. R.B.-R.: writing—review and editing, resources, formal analysis. J.E.M.-R.: writing—original draft, writing—review and editing, formal analysis. All authors have read and agreed to the published version of the manuscript.

Funding: This research was funded by Universidad Popular del Cesar, grant number 054-2019, and the APC was funded by Universidad Popular del Cesar.

Institutional Review Board Statement: Not applicable.

Informed Consent Statement: Not applicable.

Data Availability Statement: Data are contained within the article.

Conflicts of Interest: Author José Edwin Mojica-Rodríguez was employed by the company Corporación Colombiana de Investigación Agropecuaria (AGROSAVIA). The remaining authors declare that the research was conducted in the absence of any commercial or financial relationships that could be construed as a potential conflict of interest.

References

1. Kumar, V.; Goala, M.; Kumar, P.; Singh, J.; Kumar, P. Integration of treated agro-based wastewaters (TAWs) management with mushroom cultivation. In *Environmental Degradation: Causes and Remediation Strategies*; Agro Environ Media, Agriculture and Environmental Science Academy: Haridwar, India, 2020; pp. 63–75. [CrossRef]
2. Conceição, A.A.; Mendes, T.D.; Mendonça, S.; Quirino, B.F.; de Almeida, E.G.; de Siquiera, F.G. Nutraceutical Enrichment of Animal Feed by Filamentous Fungi Fermentation. *Fermentation* **2022**, *8*, 402. [CrossRef]
3. Thamvithayakorn, P.; Phosri, C.; Pisutpaisal, N.; Krajangsang, S.; Whalley, A.J.S.; Suwannasai, N. Utilization of oil palm decanter cake for valuable laccase and manganese peroxidase enzyme production from a novel white-rot fungus, *Pseudolagarobasidium* sp. PP17-33. *3 Biotech* **2019**, *9*, 417. [CrossRef] [PubMed]
4. Azzahra, Y.R.; Toharmat, T.; Prihantoro, I. Bio-processing Plantation by-products with White Oyster Mushroom (*Pleurotus ostreatus*) to Improve Fermentability and Digestibility Based on Substrate Type and Fermentation Time. *Bul. Peternak.* **2022**, *46*, 228. [CrossRef]
5. Santos, L.V.; Silva, R.R.; Silva, F.F.; Silva, J.W.D.; Barroso, D.S.; Silva, A.P.; Souza, S.O.; Santos, M.C. Increasing levels of palm kernel cake (*Elaeis guineensis* jacq.) in diets for feedlot cull cows. *Chil. J. Agric. Res.* **2019**, *79*, 628–635. [CrossRef]
6. Olukomaiya, O.; Fernando, C.; Mereddy, R.; Li, X.; Sultanbawa, Y. Solid-state fermented plant protein sources in the diets of broiler chickens: A review. *Anim. Nutr.* **2019**, *5*, 319–330. [CrossRef]
7. Oliveira, A.C.; Amorim, G.M.; Azevêdo, J.A.G.; Godoy, M.G.; Freire, D.M.G. Solid-state fermentation of co-products from palm oil processing: Production of lipase and xylanase and effects on chemical composition. *Biocatal Biotransform.* **2018**, *36*, 381–388. [CrossRef]
8. Cruz-Vázquez, A.; Tomasini, A.; Armas-Tizapantzi, A.; Marcial-Quino, J.; Montiel-González, A.M. Extracellular proteases and laccases produced by *Pleurotus ostreatus* PoB: The effects of proteases on laccase activity. *Int. Microbiol.* **2022**, *25*, 495–502. [CrossRef]
9. Nur-Nazratul, F.M.Y.; Rakib, M.R.M.; Zailan, M.Z.; Yaakub, H. Enhancing in vitro ruminal digestibility of oil palm empty fruit bunch by biological pre-treatment with *Ganoderma lucidum* fungal culture. *PLoS ONE* **2021**, *16*, e0258065. [CrossRef]
10. Boadu, K.B.; Nsiah-Asante, R.; Antwi, R.T.; Obirikorang, K.A.; Anokye, R.; Ansong, M. Influence of the chemical content of sawdust on the levels of important macronutrients and ash composition in Pearl oyster mushroom (*Pleurotus ostreatus*). *PLoS ONE* **2023**, *18*, e0287532. [CrossRef]
11. Tudzynski, B. Nitrogen regulation of fungal secondary metabolism in fungi. *Front. Microbiol.* **2014**, *5*, 656. [CrossRef]
12. Davis, M.A.; Wong, K.H. Nitrogen Metabolism in Filamentous Fungi. In *Cellular and Molecular Biology of Filamentous Fungi*; John Wiley & Sons: Hoboken, NJ, USA, 2014; pp. 325–338. [CrossRef]
13. Velásquez-Quintero, C.; Merino-Restrepo, A.; Hormaza-Anaguano, A. Production, extraction, and quantification of laccase obtained from an optimized solid-state fermentation of corncob with white-rot fungi. *J. Clean. Prod.* **2022**, *370*, 133598. [CrossRef]
14. Xu, F.; Chen, P.; Li, H.; Qiao, S.; Wang, J.; Wang, Y.; Wang, X.; Wu, B.; Liu, H.; Wang, C.; et al. Comparative transcriptome analysis reveals the differential response to cadmium stress of two *Pleurotus* fungi: *Pleurotus cornucopiae* and *Pleurotus ostreatus*. *J. Hazard. Mater.* **2021**, *416*, 125814. [CrossRef] [PubMed]
15. Fernández-Fueyo, E.; Ruiz-Dueñas, F.J.; López-Lucendo, M.F.; Pérez-Boada, M.; Rencoret, J.; Gutiérrez, A.; Pisabarro, A.G.; Ramírez, L.; Martínez, A.T. A secretomic view of woody and nonwoody lignocellulose degradation by *Pleurotus ostreatus*. *Biotechnol Biofuels* **2016**, *9*, 49. [CrossRef] [PubMed]
16. Datsomor, O.; Gou-qi, Z.; Miao, L. Effect of ligninolytic axenic and coculture white-rot fungi on rice straw chemical composition and in vitro fermentation characteristics. *Sci. Rep.* **2022**, *12*, 1129. [CrossRef]
17. Wang, Y.; Luo, Y.; Luo, L.; Zhang, H.; Liao, Y.; Gou, C. Enhancement of the nutritional value of fermented corn stover as ruminant feed using the fungi *Pleurotus* spp. *Sci. Rep.* **2021**, *11*, 11961. [CrossRef]

18. Venkateswarulu, T.C.; Prabhakar, K.V.; Kumar, R.B.; Krupanidhi, S. Modeling and optimization of fermentation variables for enhanced production of lactase by isolated *Bacillus subtilis* strain VUVD001 using artificial neural networking and response surface methodology. *3 Biotech* **2017**, *7*, 186. [CrossRef]
19. Durán-Sequeda, D.; Suspes, D.; Maestre, E.; Alfaro, M.; Pérez, G.; Ramírez, L.; Pisabarro, A.G.; Sierra, R. Effect of Nutritional Factors and Copper on the Regulation of Laccase Enzyme Production in *Pleurotus ostreatus*. *J. Fungi* **2022**, *8*, 7. [CrossRef]
20. Tinoco-Valencia, R.; Gómez-Cruz, C.; Galindo, E.; Serrano-Carreón, L. Toward an understanding of the effects of agitation and aeration on growth and laccases production by *Pleurotus ostreatus*. *J. Biotechnol.* **2014**, *177*, 67–73. [CrossRef]
21. Rubiano-Orozco, L.A.; Castro-Pacheco, A.C.; Jiménez-Rojas, F.; Fragoso-Castilla, P.J.; Ibarra-Rondón, A.J.; Rodríguez-Jiménez, D.M. Evaluación de la actividad lignocelulolítica de hongos cultivados en subproductos de la palma de aceite (*Elaeis guineensis*). *Biotecnol. Sect. Agropecu. Agroind.* **2024**, *22*, 70–86.
22. Melanouri, E.-M.; Dedousi, M.; Diamantopoulou, P. Cultivating *Pleurotus ostreatus* and *Pleurotus eryngii* mushroom strains on agro-industrial residues in solid-state fermentation. Part I: Screening for growth, endoglucanase, laccase and biomass production in the colonization pase. *Carbon Resour. Convers.* **2022**, *5*, 61–70. [CrossRef]
23. Zhou, S.; Raouche, S.; Grisel, S.; Navarro, D.; Sigoillot, J.C.; Herpoël-Gimbert, I. Solid-state fermentation in multi-well plates to assess pretreatment efficiency of rot fungi on lignocellulose biomass. *Microb. Biotechnol.* **2015**, *8*, 940–949. [CrossRef] [PubMed]
24. Cantalapiedra, C.P.; Hernández-Plaza, A.; Letunic, I.; Bork, P.; Huerta-Cepas, J. eggNOG-mapper v2: Functional Annotation, Orthology Assignments, and Domain Prediction at the Metagenomic Scale. *Mol. Biol. Evol.* **2021**, *38*, 5825–5829. [CrossRef] [PubMed]
25. Ariza Nieto, C.; Mayorga Mogollón, O.L.; Parra Forero, D.M.; Camargo Hernández, D.B.; Buitrago Albarado, C.P.; Moreno Rodríguez, J.M. *Tecnología NIRS para el Análisis Rápido y Confiable de la Composición Química de Forrajes Tropicales*; Corporación Colombiana de Investigación Agropecuaria (Agrosavia): Agustín Codazzi, Colombia, 2020. [CrossRef]
26. Minitab Inc, "Minitab® 18" [Software de Análisis Estadístico]. 2017. Available online: https://www.minitab.com/es-mx/products/minitab/ (accessed on 30 October 2024).
27. Naim, L.; Alsanad, M.A.; El Sebaaly, Z.; Shaban, N.; Abou Fayssal, S.; Sassine, Y.N. Variation of *Pleurotus ostreatus* (Jacq. Ex Fr.) P. Kumm. (1871) performance subjected to different doses and timings of nano-urea. *Saudi J. Biol. Sci.* **2020**, *27*, 1573–1579. [CrossRef] [PubMed]
28. Nunes, M.D.; Rodríguez da Luz, J.M.; Albino Paes, S.; Oliveira Ribeiro, J.J.; Soares da Silva, M.C.; Megumi Kasuya, M.C. Nitrogen Supplementation on the Productivity and the Chemical Composition of Oyster Mushroom. *J. Food Res.* **2012**, *1*, 113. [CrossRef]
29. Sassine, Y.N.; Naim, L.; El Sebaaly, Z.; Abou Fayssal, S.; Alsanad, M.A.; Yordanova, M.H. Nano urea effects on *Pleurotus ostreatus* nutritional value depending on the dose and timing of application. *Sci. Rep.* **2021**, *11*, 5588. [CrossRef]
30. Chiranjeevi, P.V.; Rajasekara, M.; Sathish, T. Enhancement of Laccase Production from *Pleurotus ostreatus* PVCRSP-7 by altering the Nutritional Conditions using Response Surface Methodology. *BioResources* **2014**, *9*, 4212–4225. [CrossRef]
31. Déo, N.; Faustin, K. Effect of substrates and doses of urea on growth and yield of an oyster mushroom (*Pleurotus ostreatus*) in greenhouse. *Int. J. Agric. Policy Res.* **2015**, *3*, 314–322. [CrossRef]
32. Sośnicka, A.; Kózka, B.; Makarova, K.; Giebułtowicz, J.; Klimaszewska, M.; Turło, J. Optimization of White-Rot Fungi Mycelial Culture Components for Bioremediation of Pharmaceutical-Derived Pollutants. *Water* **2022**, *14*, 1374. [CrossRef]
33. Haider, A.; Alam, M.M.; Khan, A.A.; Zulfiqar, M.A. Optimization of Cultural Conditions for the Treatment of Pulp and Paper Industrial Effluent by *Pleurotus ostreatus* (L.). *Pak. J. Agric. Res.* **2019**, *32*, 507–513. [CrossRef]
34. Agustin, F.; Elihasridas; Juliyarsi, I. The effect of urea supplementation and incubation time in fermentation process of bagasse by using *Ganoderma lucidum* on the growth of *G. lucidum* and the nutritive value of bagasse. *IOP Conf. Ser. Earth Environ. Sci.* **2019**, *287*, 012016. [CrossRef]
35. Daou, M.; Faulds, C.B. Glyoxal oxidases: Their nature and properties. *World J. Microbiol. Biotechnol.* **2017**, *33*, 87. [CrossRef] [PubMed]
36. Wu, Y.Y.J.; Wei, F.; Wan, Z.; Dong, Y.; Lu, Y.; Yang, P.; Jin, Y.; Saddler, J. Elucidating the synergistic action between sulfonated lignin and lytic polysaccharide monooxygenases (LPMOs) in enhancing cellulose hydrolysis. *Int. J. Biol. Macromol.* **2025**, *296*, 139674. [CrossRef]
37. Erickson, E.; Bleem, A.; Kuatsjah, E.; Werner, A.Z.; DuBois, J.L.; McGeehan, J.E.; Eltis, L.D.; Beckham, G.T. Critical enzyme reactions in aromatic catabolism for microbial lignin conversión. *Nat. Catal.* **2022**, *5*, 86–98. [CrossRef]
38. Ning, D.; Wang, H.; Ding, C.; Lu, H. Novel evidence of cytochrome P450-catalyzed oxidation of phenanthrene in *Phanerochaete chrysosporium* under ligninolytic conditions. *Biodegradation* **2010**, *21*, 889–901. [CrossRef]
39. Li, Z.; Zhao, C.; Zhou, Y.; Zheng, S.; Hu, Q.; Zou, Y. Label-free comparative proteomic analysis of *Pleurotus eryngii* grown on sawdust, bagasse, and peanut shell substrates. *J. Proteom.* **2024**, *294*, 105074. [CrossRef]
40. Li, Y.; Liu, J.; Wang, G.; Yang, M.; Yang, X.; Li, T.; Chen, G. De novo transcriptome analysis of Pleurotus djamor to identify genes encoding CAZymes related to the decomposition of corn stalk lignocellulose. *J. Biosci. Bioeng.* **2019**, *128*, 529–536. [CrossRef]

41. Xie, C.; Gong, W.; Zhu, Z.; Zhou, Y.; Xu, C.; Yan, L.; Hu, Z.; Ai, L.; Peng, Y. Comparative secretome of white-rot fungi reveals co-regulated carbohydrate-active enzymes associated with selective ligninolysis of ramie stalks. *Microb. Biotechnol.* **2021**, *14*, 911–922. [CrossRef]
42. Valadares, F.; Gonçalves, T.A.; Damasio, A.; Milagres, A.M.F.; Squina, F.M.; Segato, F.; Ferraz, A. The secretome of two representative lignocellulose-decay basidiomycetes growing on sugarcane bagasse solid-state cultures. *Enzyme Microb. Technol.* **2019**, *130*, 109370. [CrossRef]
43. Wu, H.; Nakazawa, T.; Xu, H.; Yang, R.; Bao, D.; Kawauchi, M.; Sakamoto, M.; Honda, Y. Comparative transcriptional analyses of *Pleurotus ostreatus* mutants on beech wood and rice straw shed light on substrate-biased gene regulation. *Appl. Microbiol. Biotechnol.* **2021**, *105*, 1175–1190. [CrossRef]
44. Peña, A.; Peña, A.; Babiker, R.; Chaduli, D.; Lipzen, A.; Wang, M.; Chovatia, M.; Rencoret, J.; Marques, G.; Sánchez-Ruiz, M.I.; et al. A multiomic approach to understand how *Pleurotus eryngii* transforms non-woody lignocellulosic material. *J. Fungi* **2021**, *7*, 426. [CrossRef]
45. Alfaro, M.; Oguiza, J.A.; Ramírez, L.; Pisabarro, A.G. Comparative analysis of secretomes in basidiomycete fungi. *J. Proteom.* **2014**, *6*, 28–43. [CrossRef] [PubMed]
46. Yang, Y.; Sossah, F.L.; Li, Z.; Hyde, K.D.; Li, D.; Xiao, S.; Fu, Y.; Yuan, X.; Li, Y. Genome-Wide Identification and Analysis of Chitinase GH18 Gene Family in Mycogone perniciosa. *Front. Microbiol.* **2021**, *11*, 596719. [CrossRef]
47. Yarden, O.; Zhang, J.; Marcus, D.; Changwal, C.; Mabjeesh, S.J.; Lipzen, A.; Zhang, Y.; Savage, E.; Ng, V.; Grigoriev, I.V.; et al. Altered Expression of Two Small Secreted Proteins (ssp4 and ssp6) Affects the Degradation of a Natural Lignocellulosic Substrate by *Pleurotus ostreatus*. *Int. J. Mol. Sci.* **2023**, *24*, 16828. [CrossRef]
48. Olagunju, L.K.; Isikhuemhen, O.S.; Dele, P.A.; Anike, F.N.; Essick, B.G.; Holt, N.; Udombang, N.S.; Ike, K.A.; Shaw, Y.; Brice, R.M.; et al. *Pleurotus ostreatus* Can Significantly Improve the Nutritive Value of Lignocellulosic Crop Residues. *Agriculture* **2023**, *13*, 1161. [CrossRef]
49. Sabariyah, S.; Rusdi; Damry; Hasanuddin, A. The nutritional value enhancement of oil palm empty fruit bunches as animal feed using the fungus *Coprinus comatus*, with different numbers of inoculums and incubation times. *Int. J. Des. Nat. Ecodyn.* **2021**, *16*, 269–274. [CrossRef]
50. van Dam, L.; Cruz-Morales, P.; Valerón, N.R.; de Carvalho, A.C.; Vásquez, D.P.; Lübke, M.; Pedersen, L.K.; Munk, R.; Sommer, M.O.A.; Jahn, L.J. GastronOmics: Edibility and safety of mycelium of the oyster mushroom *Pleurotus ostreatus*. *Curr. Res. Food Sci.* **2024**, *9*, 100866. [CrossRef]
51. Jaworska, G.; Berna, E. Comparison of amino acid content in canned *Pleurotus ostreatus* and *Agaricus bisporus* mushrooms. *Veg. Crops Res. Bull.* **2011**, *74*, 107–115. [CrossRef]
52. Castorina, G.; Cappa, C.; Negrini, N.; Criscuoli, F.; Casiraghi, M.C.; Marti, A.; Rollini, M.; Consonni, G.; Erba, D. Characterization and nutritional valorization of agricultural waste corncobs from Italian maize landraces through the growth of medicinal mushrooms. *Sci. Rep.* **2023**, *13*, 21148. [CrossRef]
53. Cateni, F.; Gargano, M.L.; Procida, G.; Venturella, G.; Cirlincione, F.; Ferraro, V. Mycochemicals in wild and cultivated mushrooms: Nutrition and health. *Phytochem. Rev.* **2022**, *21*, 339–383. [CrossRef]
54. Ábrego-Gacía, A.; Poggi-Varaldo, H.M.; Robles-González, V.; Ponce-Noyola, T.; Calva-Calva, G.; Ríos-Leal, E.; Estrada-Bárcenas, D.; Mendoza-Vargas, A. Lovastatin as a supplement to mitigate rumen methanogenesis: An overview. *J. Anim. Sci. Biotechnol.* **2021**, *12*, 123. [CrossRef]
55. Astudillo-Neira, R.; Suescun-Ospina, S.; Vera-Aguilera, N.; Alarcon-Enos, J.; Ávila-Stagno, J. Biodegraded hay with graded addition of *Pleurotus ostreatus* improves dry matter disappearance and reduces methane production of diets incubated in vitro. *Ital. J. Anim. Sci.* **2023**, *22*, 347–358. [CrossRef]
56. Khonkhaeng, B.; Cherdthong, A. Improving nutritive value of purple field corn residue and rice straw by culturing with white-rot fungi. *J. Fungi* **2020**, *6*, 69. [CrossRef] [PubMed]